Universality for the parameter-mismatching effect on weak synchronization in coupled chaotic systems

2004 J. Phys. A: Math. Gen. 37 8233

(http://iopscience.iop.org/0305-4470/37/34/003)

INSTITUTE OF PHYSICS PUBLISHING JOURNAL OF PHYSICS A: MATHEMATICAL AND GENERAL

J. Phys. A: Math. Gen. **37** (2004) 8233–8244 PII: S0305-4470(04)80511-0

Universality for the parameter-mismatching effect on weak synchronization in coupled chaotic systems

Woochang Lim and Sang-Yoon Kim

Department of Physics, Kangwon National University, Chunchon, Kangwon-Do 200-701, Korea

E-mail: wclim@kwnu.kangwon.ac.kr

Received 11 May 2004, in final form 15 July 2004
Published 11 August 2004
Online at stacks.iop.org/JPhysA/37/8233
doi:10.1088/0305-4470/37/34/003

Abstract

To examine the universality for the parameter-mismatching effect on weak chaotic synchronization, we study coupled multidimensional invertible systems such as the coupled Hénon maps and coupled pendula. By generalizing the method proposed in coupled one-dimensional (1D) noninvertible maps, we introduce the parameter sensitivity exponent δ to measure the degree of the parameter sensitivity of a weakly stable synchronous chaotic attractor. In terms of the parameter sensitivity exponents, we characterize the effect of the parameter mismatch on the intermittent bursting and the basin riddling occurring in the regime of weak synchronization. It is thus found that the scaling exponent μ for the average characteristic time (i.e., the average interburst time and the average chaotic transient lifetime) for both the bubbling and riddling cases is given by the reciprocal of the parameter sensitivity exponent, as in the simple system of coupled 1D maps. Hence, the reciprocal relation (i.e., $\mu = 1/\delta$) seems to be 'universal', in the sense that it holds in typical coupled chaotic systems of different nature.

PACS number: 05.45.Xt

1. Introduction

Recently, because of its potential practical applications (e.g., see [1]), the phenomenon of synchronization in coupled chaotic systems has become a field of intensive research. When identical chaotic systems synchronize, a synchronous chaotic attractor exists on an invariant subspace of the whole phase space [2]. If the synchronous chaotic attractor is stable against a perturbation transverse to the invariant subspace, it may become an attractor in the whole phase space. Such transverse stability of the synchronous chaotic attractor is intimately associated with transverse bifurcations of periodic saddles embedded in the synchronous chaotic attractor

[3–8]. If all periodic saddles are transversely stable, the synchronous chaotic attractor becomes asymptotically stable and then we have 'strong' synchronization. However, as the coupling parameter passes through a threshold value, a periodic saddle first becomes transversely unstable through a local bifurcation. After this first transverse bifurcation, trajectories may be locally repelled from the invariant subspace when they visit the neighborhood of the transversely unstable periodic repeller. Thus, we have 'weak' synchronization. For this case, intermittent bursting [9, 10] or basin riddling [11] occurs, depending on the global dynamics. If the global dynamics of the system is bounded and there are no attractors off the invariant subspace, locally repelled trajectories exhibit transient intermittent bursting. On the other hand, if the global dynamics is unbounded or there exists an attractor off the invariant subspace, repelled trajectories may go to another attractor (or infinity), and hence the basin of attraction becomes riddled with a dense set of 'holes', belonging to the basin of another attractor (or infinity).

In a real situation, a small mismatch between the subsystems that destroys the invariant synchronization subspace is unavoidable. Hence, the effect of the parameter mismatch must be taken into consideration for the study of the loss of chaos synchronization. In the regime of weak synchronization, a typical trajectory may have segments exhibiting positive local (finite-time) transverse Lyapunov exponents because of local repulsion of transversely unstable periodic repellers embedded in the synchronous chaotic attractor. For this case, any small mismatch results in a permanent intermittent bursting and a chaotic transient with a finite lifetime for the bursting and riddling cases, respectively. These attractor bubbling and chaotic transient demonstrate the sensitivity of the weakly stable synchronous chaotic attractor with respect to the variation of the mismatching parameter. Recently, we have introduced a quantifier, called the parameter sensitivity exponent, which measures the 'degree' of the parameter sensitivity in coupled one-dimensional (1D) noninvertible maps and characterized the effect of parameter mismatch on the bubbling and riddling of the weakly stable synchronous chaotic attractor [12]. Here, we extend the method of quantitatively characterizing the parameter sensitivity of the weakly stable synchronous chaotic attractor in terms of the parameter sensitivity exponent to coupled multidimensional invertible systems and examine the universality for the parameter-mismatching effect on weak synchronization.

This paper is organized as follows. In section 2, as representative models of coupled invertible systems, we consider coupled Hénon maps and coupled pendula. For each case, to measure the degree of the parameter sensitivity, we introduce the parameter sensitivity exponent, and quantitatively characterize the parameter sensitivity of the weakly stable synchronous chaotic attractor. In terms of these parameter sensitivity exponents, the effect of parameter mismatch on the attractor bubbling and basin riddling is characterized. The scaling exponent μ for the average laminar length of the bubbling attractor and the average lifetime of the chaotic transient is thus found to be given by the reciprocal of the parameter sensitivity exponent. This reciprocal relation seems to be 'universal', because it holds in typical coupled chaotic systems such as the coupled 1D maps, coupled Hénon maps and coupled pendula. Finally, we give a summary in section 3.

2. Parameter-mismatching effect in coupled invertible systems

In this section, by generalizing the method proposed in coupled 1D noninvertible maps, we introduce the parameter sensitivity exponent in the coupled Hénon maps and coupled pendula, and quantitatively characterize the parameter sensitivity of the weakly stable synchronous chaotic attractor. In terms of the parameter sensitivity exponents, the effect of parameter mismatch on the bubbling and riddling is characterized. Thus, the scaling exponent μ for the

average interburst time and the average chaotic transient lifetime is found to be given by the reciprocal of the parameter sensitivity exponent (i.e., $\mu = 1/\delta$), as in the coupled 1D maps.

2.1. Characterization of the parameter-mismatching effect in coupled Hénon maps

As a first example, we consider two coupled invertible Hénon maps, often used as a representative model for the Poincaré maps of coupled chaotic oscillators [13]:

$$T : \begin{cases} \mathbf{x}_{n+1} = \mathbf{F}(\mathbf{x}_n, \mathbf{y}_n) = \mathbf{f}(\mathbf{x}_n, a) + (1-\alpha)c\mathbf{g}(\mathbf{x}_n, \mathbf{y}_n), \\ \mathbf{y}_{n+1} = \mathbf{G}(\mathbf{x}_n, \mathbf{y}_n) = \mathbf{f}(\mathbf{y}_n, b) + c\mathbf{g}(\mathbf{y}_n, \mathbf{x}_n), \end{cases} \tag{1}$$

where $\mathbf{x}_n = \left(x_n^{(1)}, x_n^{(2)}\right)$ and $\mathbf{y}_n = \left(y_n^{(1)}, y_n^{(2)}\right)$ are state variables of the two subsystems at a discrete time n, the uncoupled dynamics ($c = 0$) is governed by the Hénon map with a nonlinearity parameter p ($p = a, b$) and a damping parameter β ($|\beta| < 1$),

$$\mathbf{f}(\mathbf{x}, p) = (f(x^{(1)}, p) - x^{(2)}, \beta x^{(1)}); \qquad f(x, p) = 1 - px^2, \tag{2}$$

c is a coupling parameter between the two subsystems, and $\mathbf{g}(\mathbf{x}, \mathbf{y})$ is a coupling function of the form

$$\mathbf{g}(\mathbf{x}, \mathbf{y}) = (g(x^{(1)}, y^{(1)}), 0); \qquad g(x, y) = y^2 - x^2. \tag{3}$$

For $\alpha = 0$, the coupling is symmetric, while for nonzero α ($0 < \alpha \leqslant 1$) it becomes asymmetric. The extreme case of asymmetric coupling with $\alpha = 1$ corresponds to the unidirectional coupling. In such a way, α tunes the degree of asymmetry in the coupling. This asymmetric coupling naturally arises in the dynamics of two clusters for the case of global coupling, in which each element is coupled to all the other elements with equal strength [13]. For the ideal case of identical Hénon maps (i.e., $a = b$), there exists an invariant synchronization plane, $x^{(1)} = y^{(1)}$ and $x^{(2)} = y^{(2)}$, in the $x^{(1)}$–$x^{(2)}$–$y^{(1)}$–$y^{(2)}$ phase space. However, in a real situation a small mismatch between the two subsystems and a small noise are unavoidable, and hence the synchronization plane is no longer invariant. Here, we restrict our attention only to the mismatching case in the absence of noise. To take into consideration such a mismatching effect, we introduce a small mismatching parameter ε in the coupled Hénon maps of equation (1) such that

$$b = a - \varepsilon. \tag{4}$$

Recently, some results on the attractor bubbling in the unidirectionally coupled case of $\alpha = 1$ have been reported in [16]. Here, as an example, we choose a mutually coupled case of $\alpha = 0.75$, and investigate both the bubbling and riddling for a fixed value of $\beta = 0.1$. For $a = 1.8$, we investigate the parameter-mismatching effect by varying the coupling parameter c. For this case a synchronous chaotic attractor exists in the interval of $c_{b,l} < c < c_{b,r}$, where $c_{b,l} = -2.3979$ and $c_{b,r} = -0.4821$. As the coupling parameter c passes $c_{b,l}$ or $c_{b,r}$, the synchronous chaotic attractor loses its transverse stability through a blowout bifurcation [13], and then a complete desynchronization occurs. In the regime of synchronization, a strongly stable synchronous chaotic attractor exists for $c_{t,l} < c < c_{t,r}$, where $c_{t,l} = -2.32$ and $c_{t,r} = -0.56$. For this case of strong synchronization, the synchronous chaotic attractor exhibits no parameter sensitivity, because all periodic saddles embedded in the synchronous chaotic attractor are transversely stable. However, as the coupling parameter c passes $c_{t,r}$ and $c_{t,l}$, bubbling and riddling transitions occur through the first transverse bifurcations of periodic saddles, respectively [7, 8], and then we have weak synchronization. For this case, the weakly stable synchronous chaotic attractor has a parameter sensitivity, because of local transverse repulsion of the periodic repellers embedded in the synchronous chaotic attractor. Hence, however small the parameter mismatching ε, a persistent intermittent bursting, called

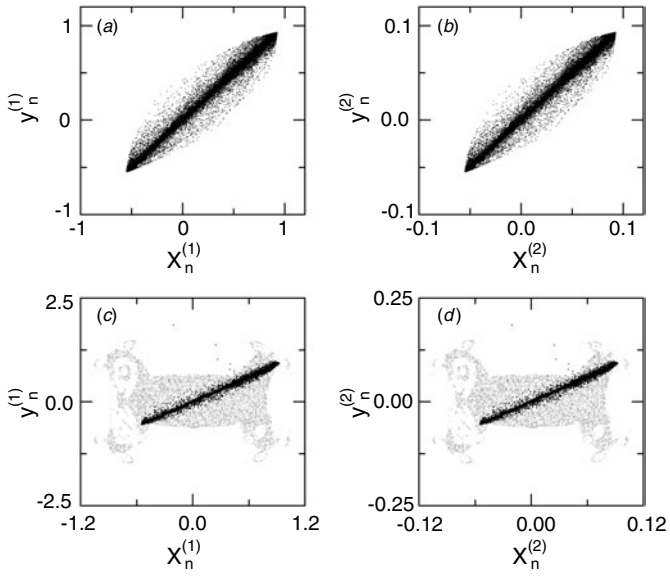

Figure 1. Effect of parameter mismatch with $\varepsilon = 0.002$ on weak synchronization for $a = 1.8$ in mutually coupled Hénon maps with $\alpha = 0.75$. For $c = -0.49$, projections of a bubbling attractor onto the (a) $x^{(1)}$–$y^{(1)}$ and (b) $x^{(2)}$–$y^{(2)}$ planes are given. In both (a) and (b), the initial orbit point is $(x^{(1)}, x^{(2)}, y^{(1)}, y^{(2)}) = (0.7, 0.07, 0.7, 0.07)$, the 5×10^3 points are computed before plotting and the next 4×10^4 points are plotted. For the riddling case of $c = -2.39$, the synchronous chaotic attractor with a basin (grey region) riddled with a dense set of 'holes' leading to divergent trajectories (white region) for $\varepsilon = 0$ is transformed into a chaotic transient (black dots). In (c) (d), a 2D slice with $x^{(2)} = y^{(2)} = 0.05$ ($x^{(1)} = y^{(1)} = 0.5$) through the 4D riddled basin of the weakly stable synchronous chaotic attractor is shown. Projections of a chaotic transient starting from an initial orbit point $(x^{(1)}, x^{(2)}, y^{(1)}, y^{(2)}) = (0.7, 0.07, 0.7, 0.07)$ onto the (c) $x^{(1)}$–$y^{(1)}$ and (d) $x^{(2)}$–$y^{(2)}$ planes are given.

the attractor bubbling, occurs in the regime of bubbling ($c_{t,r} < c < c_{b,r}$). Figures 1(a) and (b) show such attractor bubbling for $c = -0.49$ and $\varepsilon = 0.002$. On the other hand, in the regime of riddling ($c_{b,l} < c < c_{t,l}$), the weakly stable synchronous chaotic attractor with a riddled basin for $\varepsilon = 0$ is transformed into a chaotic transient (denoted by black dots) with a finite lifetime in the presence of parameter mismatch, as shown in figures 1(c) and (d) for $c = -2.39$. As c is changed away from $c_{t,l}$ or $c_{t,r}$, transversely unstable periodic repellers appear successively in the synchronous chaotic attractor via transverse bifurcations. Then, the degree of the parameter sensitivity of the synchronous chaotic attractor increases, because of the increase in the strength of local transverse repulsion of the periodic repellers embedded in the synchronous chaotic attractor.

We generalize the method proposed in the coupled 1D maps [12] to the case of the coupled Hénon maps and quantitatively characterize the parameter sensitivity of the synchronous chaotic attractor as follows. As the strength of the local transverse repulsion from the synchronization plane increases, the synchronous chaotic attractor becomes more and more sensitive with respect to the variation of ε. Such parameter sensitivity of the synchronous chaotic attractor for $\varepsilon = 0$ may be characterized by calculating the derivative of the transverse variable $\mathbf{u}_n = \mathbf{x}_n - \mathbf{y}_n$, denoting the deviation from the synchronization plane, with respect to ε $\left(\text{i.e. } \frac{\partial \mathbf{u}_{n+1}}{\partial \varepsilon}\Big|_{\varepsilon=0} = \frac{\partial \mathbf{x}_{n+1}}{\partial \varepsilon}\Big|_{\varepsilon=0} - \frac{\partial \mathbf{y}_{n+1}}{\partial \varepsilon}\Big|_{\varepsilon=0}\right)$. Using equation (1), we may obtain the following

recurrence relation,

$$\left.\frac{\partial \mathbf{u}_{n+1}}{\partial \varepsilon}\right|_{\varepsilon=0} = r(\mathbf{x}_n^*)\left.\frac{\partial \mathbf{u}_n}{\partial \varepsilon}\right|_{\varepsilon=0} + \mathbf{f}_a(\mathbf{x}_n^*, a), \tag{5}$$

where $\left.\frac{\partial \mathbf{u}_n}{\partial \varepsilon}\right|_{\varepsilon=0} = \left(\left.\frac{\partial u_n^{(1)}}{\partial \varepsilon}\right|_{\varepsilon=0}, \left.\frac{\partial u_n^{(2)}}{\partial \varepsilon}\right|_{\varepsilon=0}\right)$, the 2×2 matrix $r(\mathbf{x}_n^*)$ is given by

$$r(\mathbf{x}_n^*) \equiv \begin{pmatrix} f_{x^{(1)}}\left(x_n^{(1)*}, a\right) - (2-\alpha)ch\left(x_n^{(1)*}\right) & -1 \\ \beta & 0 \end{pmatrix}, \tag{6}$$

and

$$\mathbf{f}_a(\mathbf{x}_n^*, a) = \begin{pmatrix} f_a\left(x_n^{(1)*}, a\right) \\ 0 \end{pmatrix}. \tag{7}$$

Here, f_x and f_a are the derivatives of $f(x, a)$ with respect to x and a, $\{(\mathbf{x}_n^*, \mathbf{y}_n^*)\}$ is a synchronous orbit with $\mathbf{x}_n^* = \mathbf{y}_n^*$ for $\varepsilon = 0$, and $h(x)$ is a reduced coupling function defined by [14]

$$h(x) \equiv \left.\frac{\partial g(x, y)}{\partial y}\right|_{y=x}. \tag{8}$$

Hence, starting from an initial orbit point $(\mathbf{x}_0^*, \mathbf{y}_0^*)$ on the synchronization plane, we may obtain derivatives at all points of the orbit:

$$\left.\frac{\partial \mathbf{u}_N}{\partial \varepsilon}\right|_{\varepsilon=0} = \sum_{k=1}^{N} R_{N-k}(\mathbf{x}_k^*)\mathbf{f}_a(\mathbf{x}_{k-1}^*, a) + R_N(\mathbf{x}_0^*)\left.\frac{\partial \mathbf{u}_0}{\partial \varepsilon}\right|_{\varepsilon=0}, \tag{9}$$

where

$$R_M(\mathbf{x}_m^*) = \prod_{i=0}^{M-1} r(\mathbf{x}_{m+i}^*), \tag{10}$$

which is a product of the 'transverse Jacobian matrices' $r(\mathbf{x}^*)$ determining the stability against a perturbation transverse to the synchronization plane and $R_0 = I$ (identity matrix). Note that the eigenvalues, $\lambda_M^{T,1}(\mathbf{x}_m^*)$ and $\lambda_M^{T,2}(\mathbf{x}_m^*)$ $\left(\left|\lambda_M^{T,1}(\mathbf{x}_m^*)\right| \geqslant \left|\lambda_M^{T,2}(\mathbf{x}_m^*)\right|\right)$, of $R_M(\mathbf{x}_m^*)$ are associated with local (M-time) transverse Lyapunov exponents $\sigma_M^{T,1}$ and $\sigma_M^{T,2}$ $\left(\sigma_M^{T,1} \geqslant \sigma_M^{T,2}\right)$ of the synchronous chaotic attractor that are averaged over M synchronous orbit points starting from $\mathbf{x}_m^*$ as follows:

$$\sigma_M^{T,i}(\mathbf{x}_m^*) = \frac{1}{M}\ln\left|\lambda_M^{T,i}(\mathbf{x}_m^*)\right| \qquad (i = 1, 2). \tag{11}$$

Thus, $\lambda_M^{T,1}$ and $\lambda_M^{T,2}$ become local (transverse stability) multipliers that determine local sensitivity of the motion during a finite time M. As $M \to \infty$, $\sigma_M^{T,1}$ approaches the largest transverse Lyapunov exponent $\sigma_T^{(1)}$ that denotes the average exponential rate of divergence of an infinitesimal perturbation transverse to the synchronous chaotic attractor. Because the initial point (x_0^*, y_0^*) starts on the synchronization plane (i.e., $x_0^* = y_0^*$), the value of the initial transverse variable $\mathbf{u}_0 = \mathbf{x}_0^* - \mathbf{y}_0^*$ is always zero, independently of ε $\left(\text{i.e.}, \left.\frac{\partial \mathbf{u}_0}{\partial \varepsilon}\right|_{\varepsilon=0} = 0\right)$. Hence, equation (9) reduces to

$$\left.\frac{\partial \mathbf{u}_N}{\partial \varepsilon}\right|_{\varepsilon=0} = \mathbf{S}_N(\mathbf{x}_0^*) \equiv \sum_{k=1}^{N} R_{N-k}(\mathbf{x}_k^*)\mathbf{f}_a(\mathbf{x}_{k-1}^*, a). \tag{12}$$

Since the values of $\mathbf{f}_a$ are bounded, the boundedness of the partial sum $\mathbf{S}_N$ is determined just by the largest eigenvalues $\lambda_M^{T,1}$ of R_M.

For the case of weak synchronization, there are transversely unstable periodic repellers embedded in the synchronous chaotic attractor. When a typical trajectory visits

neighbourhoods of such repellers, it has segments experiencing local repulsion from the synchronization plane. Thus, the distribution of largest local transverse Lyapunov exponents $\sigma_M^{T,1}$ for a large ensemble of trajectories and for large M may have a positive tail [12]. For the segments of a trajectory exhibiting a positive largest local transverse Lyapunov exponent $\left(\sigma_M^{T,1} > 0\right)$, the largest local transverse multipliers $\lambda_M^{T,1}\left(= \pm \exp\left(\sigma_M^{T,1} M\right)\right)$ can be arbitrarily large, and hence the partial sums $S_N^{(i)}$ $(i = 1, 2)$ may be arbitrarily large. This implies unbounded growth of the derivatives $\frac{\partial u_N^{(i)}}{\partial \varepsilon}\big|_{\varepsilon=0}$ $(i = 1, 2)$ as N tends to infinity, and consequently the weakly stable synchronous chaotic attractor may have a parameter sensitivity.

As an example, we consider the case of weak synchronization in the mutually coupled case of $\alpha = 0.75$ for $c = -0.49$. If we iterate equation (5) with $\frac{\partial \mathbf{u}_0}{\partial \varepsilon}\big|_{\varepsilon=0} = 0$ along a synchronous trajectory starting from an initial orbit point $(\mathbf{x}_0^*, \mathbf{y}_0^*)$ on the synchronization plane, then we obtain the partial sum $\mathbf{S}_N(\mathbf{x}_0^*)$ of equation (12). The partial sum $S_N^{(i)}$ $\left(= \frac{\partial u_N^{(i)}}{\partial \varepsilon}\big|_{\varepsilon=0}\right)$ $(i = 1, 2)$ becomes very intermittent. However, by looking only at the maximum

$$\gamma_N^{(i)}(x_0^*) = \max_{0 \leqslant n \leqslant N} \left| S_n^{(i)}(\mathbf{x}_0^*) \right| \qquad (i = 1, 2), \tag{13}$$

one can easily see the boundedness of $S_N^{(i)}$. For this case, $\gamma_N^{(1)}$ and $\gamma_N^{(2)}$ grow unboundedly, and hence the weakly stable synchronous chaotic attractor has a parameter sensitivity. The growth rate of the function $\gamma_N^{(i)}(\mathbf{x}_0^*)$ with time N represents a degree of the parameter sensitivity, and can be used as a quantitative characteristic of the weakly stable synchronous chaotic attractor. However, $\gamma_N^{(i)}(\mathbf{x}_0^*)$ depends on a particular trajectory. To obtain a 'representative' quantity that is independent of a particular trajectory, we consider an ensemble of randomly chosen initial points $(\mathbf{x}_0^*, \mathbf{y}_0^*)$ on the synchronization plane, and take the minimum value of $\gamma_N^{(i)}$ with respect to the initial orbit points,

$$\Gamma_N^{(i)} = \min_{\mathbf{x}_0^*} \gamma_N^{(i)}(\mathbf{x}_0^*) \qquad (i = 1, 2). \tag{14}$$

While other representative quantities may be defined (e.g., the average of γ_N over an ensemble of trajectories), the numerical convergence for the case of minimum value is better than that for other cases, and hence we choose the minimum value as a representative one, as in the case of the phase sensitivity exponent in the quasiperiodically forced systems [17]. Figure 2(*a*) shows parameter sensitivity functions $\Gamma_N^{(1)}$ and $\Gamma_N^{(2)}$, which are obtained in an ensemble containing 100 random initial orbit points. The unbounded growth of both $\Gamma_N^{(1)}$ and $\Gamma_N^{(2)}$ is determined by the same largest local transverse multiplier $\lambda_M^{T,1}$ (i.e., the largest eigenvalue of R_M in equation (10)). Hence, they grow unboundedly with the same power δ,

$$\Gamma_N^{(i)} \sim N^{\delta} \qquad \text{for} \quad i = 1, 2. \tag{15}$$

Here, the value of $\delta \simeq 4.6$ is a quantitative characteristic of the parameter sensitivity of the synchronous chaotic attractor for $c = -0.49$, and we call it the parameter sensitivity exponent.

In each regime of bubbling or riddling, we obtain the parameter sensitivity exponents by changing the coupling parameter c from the bubbling or riddling transition point to the blowout bifurcation point. However, the value of the parameter sensitivity exponent obtained in an ensemble containing 100 random initial points fluctuates a little, depending on the chosen ensemble. Hence, it is necessary to consider many ensembles for obtaining a better statistics. From our extensive numerical simulations, we find that it is enough to consider about 100 ensembles for each c, each of which contains 100 randomly chosen initial orbit points. Thus, we choose the average value of the 100 parameter sensitivity exponents obtained in the 100 ensembles. Figure 2(*b*) shows the plot of such averaged parameter sensitivity

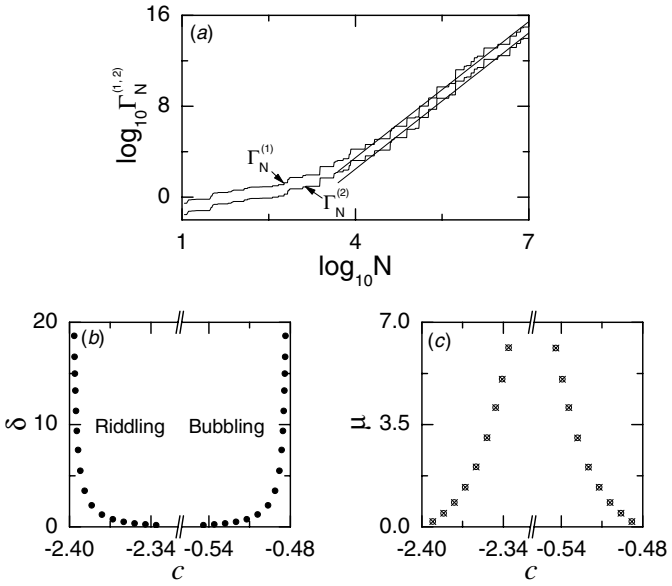

Figure 2. Parameter sensitivity for $a = 1.8$ in mutually coupled Hénon maps with $\alpha = 0.75$. Parameter sensitivity functions $\Gamma_N^{(1)}$ and $\Gamma_N^{(2)}$, exhibiting asymptotic power-law behaviours, are shown in (*a*) for $c = -0.49$. They are well fitted with straight lines with the slope $\delta \simeq 4.6$. (*b*) Plot of the parameter sensitivity exponents δ (solid circles) versus c. (*c*) Plot of the scaling exponents μ (open circles) for the average characteristic time versus c. They agree well with the reciprocal of the parameter sensitivity exponents (crosses).

exponents (denoted by solid circles) versus c. Note that the parameter sensitivity exponent δ monotonically increases as c is varied away from the bubbling or riddling transition point, and tends to infinity as c approaches the blowout bifurcation point. This increase in the parameter sensitivity of the synchronous chaotic attractor is caused by the increase in the strength of local transverse repulsion of periodic repellers embedded in the synchronous chaotic attractor. After the blowout bifurcation, the weakly stable synchronous chaotic attractor becomes transversely unstable, and hence a complete desynchronization occurs.

In terms of the parameter sensitivity exponents, we characterize the parameter-mismatching effect on the bubbling and riddling of a weakly stable synchronous chaotic attractor. In the presence of parameter match, the weakly stable synchronous chaotic attractor is transformed into a bubbling attractor or a chaotic transient, depending on the global dynamics. For this case the quantity of interest is the average time τ spent near the synchronization plane. For the case of the bubbling attractor, τ is the average interburst time, while for the case of the chaotic transient, τ is its average lifetime. As c is varied from the bubbling or riddling transition point, τ becomes short because the strength of local transverse repulsion of periodic repellers embedded in the synchronous chaotic attractor increases.

For the case of bubbling, a typical trajectory on the bubbling attractor exhibits a persistent intermittent bursting, in which long episodes of nearly synchronous evolution are occasionally interrupted by short-term bursts. To characterize the intermittent bursting, we use a small quantity d_b^* for the threshold value of the magnitude of the deviation from the synchronization plane, $d_n \left(\equiv \left(\left|u_n^{(1)}\right| + \left|u_n^{(2)}\right|\right)/2\right)$, such that for $d_n < d_b^*$ the bubbling attractor is in the laminar phase, where a typical trajectory exhibits nearly synchronous motion, and for $d_n \geqslant d_b^*$ it is in the bursting phase. Here d_b^* is very small compared to the maximum bursting amplitude

and it is the maximum deviation from the synchronization plane that may be acceptable in the context of synchronization. For each c, we follow a trajectory starting from a random initial orbit point until 50 000 laminar phases are obtained, and then we get the average laminar length τ (i.e., the average interburst interval) that scales with ε as [15]

$$\tau \sim \varepsilon^{-\mu}. \tag{16}$$

The plot of μ (denoted by open circles) versus c is shown in figure 2(c). As c increases, the value of μ decreases, because the average laminar length shortens.

For each c in the regime of riddling, we consider an ensemble of trajectories starting from 1000 randomly chosen initial points on the synchronization plane and obtain the average lifetime of the chaotic transients. A trajectory may be regarded as having escaped once the magnitude of deviation d_n from the synchronization plane becomes larger than a threshold value d_c^* such that an orbit point with $d > d_c^*$ lies sufficiently outside the basin of the synchronous chaotic attractor. Thus, the average lifetime τ is found to exhibit a power-law scaling behaviour as in equation (16). The plot of the scaling μ (denoted by open circles) versus c is given in figure 2(c). As c decreases toward the blowout bifurcation point, the average lifetime shortens, and hence the value of μ decreases.

For both the bubbling and riddling cases, a reciprocal relation between the the scaling exponent μ and the parameter sensitivity exponent δ is derived and numerically confirmed. For a given ε, consider a trajectory starting from a randomly chosen initial orbit point on the synchronization plane. Then, from equations (12)–(15) the 'average' deviation of the trajectory from the synchronization plane after N iterations can be obtained for sufficiently small ε:

$$d_N = \tfrac{1}{2}\left(\left|u_N^{(1)}\right| + \left|u_N^{(2)}\right|\right) \sim \left(\Gamma_N^{(1)} + \Gamma_N^{(2)}\right)\varepsilon \sim N^{\delta}\varepsilon. \tag{17}$$

Then, the 'average' characterization time τ at which the magnitude of the deviation d_τ becomes the threshold value $d_{b,c}^*$ (i.e., $d_\tau = d_{b,c}^*$) is given by

$$\tau \sim \varepsilon^{-1/\delta}. \tag{18}$$

Hence, the scaling exponent μ for τ becomes just the reciprocal of the parameter sensitivity exponent δ,

$$\mu = 1/\delta, \tag{19}$$

as in the case of the coupled 1D maps [12]. To confirm the reciprocal relation, the reciprocal values of numerically obtained δ (denoted by crosses) are plotted in figure 2(c), and we note that they agree well with the values of μ (denoted by open circles).

2.2. Characterization of the parameter-mismatching effect in coupled pendula

As a second example, we consider an invertible system of two coupled parametrically forced pendula [13]:

$$\begin{aligned} \dot{\mathbf{x}} &= \mathbf{F}(\mathbf{x}, \mathbf{y}) = \mathbf{f}(\mathbf{x}, a) + (1-\alpha)c\mathbf{g}(\mathbf{x}, \mathbf{y}), \\ \dot{\mathbf{y}} &= \mathbf{G}(\mathbf{x}, \mathbf{y}) = \mathbf{f}(\mathbf{y}, b) + c\mathbf{g}(\mathbf{y}, \mathbf{x}), \end{aligned} \tag{20}$$

where the overdot denotes the differentiation with respect to the time, $\mathbf{x} = (x^{(1)}, x^{(2)})$ and $\mathbf{y} = (y^{(1)}, y^{(2)})$ are state variables of the two subsystems, c is a coupling parameter between the subsystems, α ($0 \leqslant \alpha \leqslant 1$) is a parameter tuning the degree of the asymmetry of coupling and $\mathbf{g}(\mathbf{x}, \mathbf{y})$ is a coupling function of the form,

$$\mathbf{g}(\mathbf{x}, \mathbf{y}) = (g(x^{(1)}, y^{(1)}), g(x^{(2)}, y^{(2)})); \qquad g(x, y) = y - x. \tag{21}$$

Here, the uncoupled dynamics ($c = 0$) is governed by a parametrically forced pendulum,

$$\begin{aligned} &\mathbf{f}(\mathbf{x}, p) = (x^{(2)}, f(x^{(1)}, x^{(2)}, p)); \\ &f(x^{(1)}, x^{(2)}, p) = -2\pi\beta\Omega x^{(2)} - 2\pi(\Omega^2 - p\cos 2\pi t)\sin 2\pi x^{(1)}, \end{aligned} \tag{22}$$

where $x^{(1)}$ is a normalized angle with range $x^{(1)} \in [0, 1)$, $x^{(2)}$ is a normalized angular velocity, β is a normalized damping parameter, Ω is a normalized natural frequency of the unforced pendulum, $p\,(p = a, b)$ is a normalized driving amplitude of the vertical oscillation of the suspension point. As in two coupled Hénon maps, these two coupled pendula may also be used as a model for investigating the two-cluster dynamics in many globally coupled pendula.

The phase space of the coupled parametrically forced pendula is five-dimensional with coordinates $x^{(1)}, x^{(2)}, y^{(1)}, y^{(2)}$ and t. Since the system is periodic in t, it is convenient to regard time as a circular coordinate in the phase space. We also consider the surface of section, the $x^{(1)}$–$x^{(2)}$–$y^{(1)}$–$y^{(2)}$ hypersurface at integer times (i.e., $t = m, m$: integer). Then, using the fourth-order Runge–Kutta method with a time step $h = 0.05$, we integrate equation (20) and follow a trajectory. This phase-space trajectory intersects the surface of section in a sequence of points. This sequence of points corresponds to a mapping on the 4D hypersurface. The map can be computed by stroboscopically sampling the orbit points $\mathbf{z}_m \equiv (x^{(1)}(m), x^{(2)}(m), y^{(1)}(m), y^{(2)}(m))$ at the discrete time m. We call the transformation $\mathbf{z}_m \to \mathbf{z}_{m+1}$ the Poincaré map and write $\mathbf{z}_{m+1} = P(\mathbf{z}_m)$. This 4D Poincaré map P has a constant Jacobian determinant of $\mathrm{e}^{-4\pi\beta\Omega-(4-2\alpha)c}$.

As an example, we consider the 4D Poincaré map P for the unidirectionally coupled case of $\alpha = 1$ and fix the values of β and Ω at $\beta = 1.0$ and $\Omega = 0.5$. For the ideal case without parameter mismatch (i.e., $a = b$), there exists an invariant synchronization plane, $x^{(1)} = y^{(1)}$ and $x^{(2)} = y^{(2)}$, in the $x^{(1)}$–$x^{(2)}$–$y^{(1)}$–$y^{(2)}$ phase space. However, in a real situation the parameter mismatch between the two subsystems is unavoidable, and hence the synchronization plane is no longer invariant. To take into consideration such a mismatching effect, we introduce a small mismatching parameter ε such that $b = a - \varepsilon$.

For $a = 0.85$, we investigate the parameter-mismatching effect by varying the coupling parameter c. For this case an synchronous chaotic attractor exists for $c > c_b \simeq 0.648$. As the coupling parameter c passes c_b, the synchronous chaotic attractor loses its transverse stability through a blowout bifurcation, and then a complete desynchronization occurs. In the regime of synchronization, a strongly stable synchronous chaotic attractor without parameter sensitivity exists for $c > c_t = 0.858\,688$, because all periodic saddles embedded in the synchronous chaotic attractor are transversely stable. However, as the coupling parameter c passes c_t, a bubbling transition occurs through the first transverse bifurcation of a periodic saddle, and then we have weak synchronization. Hence, only the attractor bubbling occurs in the regime of weak synchronization ($c_b < c < c_t$), as shown in figures 3(a) and (b) for $c = 0.67$ and $\varepsilon = 0.0001$. For this case, the weakly stable synchronous chaotic attractor exhibits a parameter sensitivity, because of local transverse repulsion of the periodic repellers embedded in the synchronous chaotic attractor.

Such parameter sensitivity of the weakly stable synchronous chaotic attractor for $\varepsilon = 0$ may be characterized by calculating the derivative of the transverse variable $\mathbf{u} = \mathbf{x} - \mathbf{y}$, denoting the deviation from the synchronization plane, with respect to ε $\left(\text{i.e. } \frac{\partial \mathbf{u}}{\partial \varepsilon}\Big|_{\varepsilon=0} = \frac{\partial \mathbf{x}}{\partial \varepsilon}\Big|_{\varepsilon=0} - \frac{\partial \mathbf{y}}{\partial \varepsilon}\Big|_{\varepsilon=0}\right)$. Using equation (20), we may obtain the following governing equation for $\frac{\partial \mathbf{u}}{\partial \varepsilon}\Big|_{\varepsilon=0}$,

$$\left.\frac{\partial \dot{\mathbf{u}}}{\partial \varepsilon}\right|_{\varepsilon=0} = r(\mathbf{x}^*)\left.\frac{\partial \mathbf{u}}{\partial \varepsilon}\right|_{\varepsilon=0} + \mathbf{f}_a(\mathbf{x}^*, a), \tag{23}$$

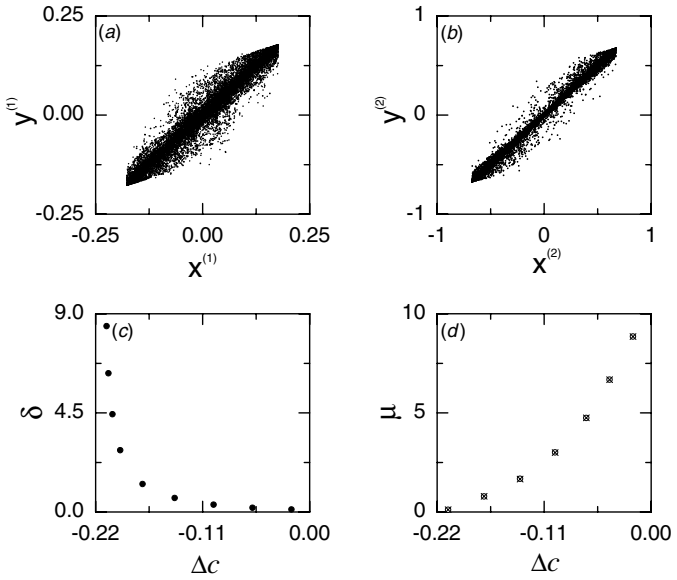

Figure 3. Effect of parameter mismatch on weak synchronization for $a = 0.85$ in the 4D Poincaré map of unidirectionally coupled pendula. For $c = 0.67$ and $\varepsilon = 0.0001$, projections of a bubbling attractor onto the (*a*) $x^{(1)}$–$y^{(1)}$ and (*b*) $x^{(2)}$–$y^{(2)}$ planes are given. In both (*a*) and (*b*), the initial orbit point is $(x^{(1)}, x^{(2)}, y^{(1)}, y^{(2)}) = (0.1, 0.3, 0.1, 0.3)$, the 5×10^3 points are computed before plotting and the next 5×10^4 points are plotted. (*c*) Plot of the parameter sensitivity exponents δ (solid circles) versus $\Delta c = c - c_t$ for $a = 0.85$. (*d*) Plot of the scaling exponents μ (open circles) for the average interburst interval versus Δc for $a = 0.85$. They agree well with the reciprocal of the parameter sensitivity exponents (crosses).

where $\frac{\partial \mathbf{u}}{\partial \varepsilon}\big|_{\varepsilon=0} = \left(\frac{\partial u^{(1)}}{\partial \varepsilon}\big|_{\varepsilon=0}, \frac{\partial u^{(2)}}{\partial \varepsilon}\big|_{\varepsilon=0}\right)$, the 2×2 matrix $r(\mathbf{x}^*)$ is given by

$$r(\mathbf{x}^*) \equiv \begin{pmatrix} -(2-\alpha)ch(x^{(1)*}) & 1 \\ f_{x^{(1)}}(x^{(1)}, x^{(2)}, a) & f_{x^{(2)}}(x^{(1)}, x^{(2)}, a) - (2-\alpha)ch(x^{(2)*}) \end{pmatrix}, \quad (24)$$

and

$$\mathbf{f}_a(\mathbf{x}^*, a) = \begin{pmatrix} 0 \\ f_a(x^{(1)}, x^{(2)}, a) \end{pmatrix}. \quad (25)$$

Here, $f_{x^{(1)}}$, $f_{x^{(2)}}$ and f_a are the derivatives of $f(x^{(1)}, x^{(2)}, a)$ with respect to $x^{(1)}, x^{(2)}$ and a, $\{(\mathbf{x}_n^*, \mathbf{y}_n^*)\}$ is a synchronous orbit with $\mathbf{x}_n^* = \mathbf{y}_n^*$ for $\varepsilon = 0$, and $h(x) \equiv \frac{\partial g(x,y)}{\partial y}\big|_{y=x}$ is a reduced coupling function. Integrating the formula (23) along a synchronous trajectory starting from an initial orbit point $(\mathbf{x}_0^*, \mathbf{y}_0^*)$ on the synchronization plane and an initial value $\frac{\partial \mathbf{u}}{\partial \varepsilon}\big|_{\varepsilon=0} = \mathbf{0}$ for $t = 0$, we may obtain derivatives $\mathbf{S}_n(\mathbf{x}^*) \equiv \frac{\partial \mathbf{u}}{\partial \varepsilon}\big|_{\varepsilon=0}$ at all subsequent discrete time $t = n$. Then, following the same procedure as in the coupled Hénon maps, one can obtain the parameter sensitivity exponent δ of equation (15) which measures the degree of parameter sensitivity of the synchronous chaotic attractor.

In the regime of bubbling, we obtain the parameter sensitivity exponents by changing the coupling parameter c from the bubbling transition point c_t to the blowout bifurcation point c_b. As in the case of coupled Hénon maps, for obtaining satisfactory statistics, we consider 100 ensembles for each c, each of which contains 20 randomly chosen initial orbit points on the synchronization plane and choose the average value of the 100 parameter sensitivity exponents obtained in the 100 ensembles. Figure 3(*c*) shows the plot of such parameter

sensitivity exponents (denoted by solid circles) versus $\Delta c \equiv c - c_t$. Note that the parameter sensitivity exponent δ monotonically increases as c is varied away from the bubbling transition point and tends to infinity as c approaches the blowout bifurcation point. This increase in the parameter sensitivity of the synchronous chaotic attractor is caused by the increase in the strength of local transverse repulsion of periodic repellers embedded in the synchronous chaotic attractor.

In terms of the parameter sensitivity exponents, we characterize the parameter-mismatching effect on the bubbling of a weakly stable synchronous chaotic attractor. For each c, we follow a trajectory starting from a random initial orbit point until 50 000 laminar phases are obtained, and then we find that the average laminar length τ exhibits a power-law scaling behaviour as in equation (16). The plot of the scaling exponent μ (denoted by open circles) versus $\Delta c \equiv c - c_t$ is shown in figure 3(d). As c decreases from c_t, the value of μ decreases, because the average laminar length shortens. As in the case of coupled Hénon maps, the scaling exponent μ is given by the reciprocal of the parameter sensitivity exponent δ (see equation (19)). To examine the reciprocal relation, the reciprocal values of numerically obtained δ (denoted by crosses) are plotted in figure 3(d). Note that they agree well with the values of μ (denoted by open circles), as in the preceding example of coupled Hénon maps.

So far, in both systems of mutually coupled Hénon maps with $\alpha = 0.75$ and unidirectionally coupled pendula with $\alpha = 1$, we have characterized the parameter-mismatching effect. Through equation (6) (equation (24)), one can easily see that the parameter sensitivity exponent for a given (a, c) in the case of $\alpha = 0.75$ ($\alpha = 1$) is the same as that for the value of $[a, 1.25c/(2-\alpha)]$ ($[a, c/(2-\alpha)]$) for any other case of α. Thus, the results of the parameter sensitivity exponents given in figure 2(b) (figure 3(c)) may be converted into those for the case of general α only by a scale change in the coupling parameter such that $c \to 1.25c/(2-\alpha)$ $[c \to c/(2-\alpha)]$.

3. Summary

To examine the universality for the parameter-mismatching effect on weak synchronization, we have studied the coupled Hénon maps and coupled pendula which are multidimensional invertible systems. By extending the method proposed in coupled 1D noninvertible maps, we have investigated the parameter sensitivity of a weakly stable synchronous chaotic attractor. For the case of coupled Hénon maps and pendula, there exist two parameter sensitivity functions, $\Gamma_N^{(i)}$ ($i = 1, 2$). However, the unbounded growth of both $\Gamma_N^{(1)}$ and $\Gamma_N^{(2)}$ is governed by the same largest local transverse multiplier $\lambda_M^{T,1}$ (i.e., the largest eigenvalue of R_M in equation 10)). Hence, they grow unboundedly with the same parameter sensitivity exponent δ $\left(\text{i.e., } \Gamma_N^{(i)} \sim N^{\delta}\right)$. In the regime of weak synchronization, we have numerically obtained the parameter sensitivity exponents by changing the coupling parameter and quantitatively characterized the parameter sensitivity of the weakly stable synchronous chaotic attractor. In terms of these parameter sensitivity exponents, the parameter-mismatching effect on the scaling behaviour, associated with the average laminar length and the average chaotic transient lifetime, has been investigated. For this case, the reciprocal relation between the scaling exponent μ and the parameter sensitivity exponent (i.e., $\mu = 1/\delta$) has been derived and numerically confirmed. Hence, it is conjectured that the reciprocal relation might be 'universal', because it holds in typical coupled chaotic systems such as the coupled 1D maps, coupled Hénon maps and coupled pendula. For more complete examination of the universality, further numerical works in several other kinds of coupled systems and rigorous mathematical works are required. However, this subject is beyond the scope of the present work, and is left for future work.

Acknowledgment

This work was supported by the Korea Science and Engineering Foundation (grant no. R05-2003-000-10045-0).

References

[1] Cuomo K M and Oppenheim A V 1993 *Phys. Rev. Lett.* **71** 65
Kocarev L, Halle K S, Eckert K, Chua L O and Parlitz U 1992 *Int. J. Bifurcation Chaos Appl. Sci. Eng.* **2** 973
Kocarev L and Parlitz U 1995 *Phys. Rev. Lett.* **74** 5028
Rulkov N F 1996 *Chaos* **6** 262
[2] Fujisaka H and Yamada T 1983 *Prog. Theor. Phys.* **69** 32
Pikovsky A S 1984 *Z. Phys. B: Condens. Matter* **50** 149
Afraimovich V S, Verichev N N and Rabinovich M I 1986 *Radiophys. Quantum Electron.* **29** 795
Pecora L M and Carroll T L 1990 *Phys. Rev. Lett.* **64** 821
[3] Ashwin P, Buescu J and Stewart I 1996 *Nonlinearity* **9** 703
[4] Hunt B R and Ott E 1996 *Phys. Rev. Lett.* **76** 2254
Hunt B R and Ott E 1996 *Phys. Rev.* E **54** 328
[5] Lai Y-C, Grebogi C, Yorke J A and Venkataramani S C 1996 *Phys. Rev. Lett.* **77** 55
[6] Astakhov V, Shabunin A, Kapitaniak T and Anishchenko V 1996 *Phys. Rev. Lett.* **77** 55
[7] Maistrenko Yu L, Maistrenko V L, Popovich O and Mosekilde E 1998 *Phys. Rev.* E **57** 2713
Maistrenko Yu L, Maistrenko V L, Popovich O and Mosekilde E 1999 *Phys. Rev.* E **60** 2817
Popovych O, Yu Maistrenko L, Mosekilde E, Pikovsky A and Kurths J 2001 *Phys. Rev.* E **63** 036201
[8] Kim S-Y and Lim W 2001 *Phys. Rev.* E **63** 026217
Kim S-Y and Lim W 2001 *Phys. Rev.* E **64** 016211
Kim S-Y and Lim W 2003 *J. Phys.* A **36** 6951
Kim S-Y, Lim W and Kim Y 2001 *Prog. Theor. Phys.* **105** 187
[9] Ashwin P, Buescu J and Stewart I 1994 *Phys. Lett.* A **193** 126
Heagy J F, Carroll T L and Pecora L M 1995 *Phys. Rev.* E **52** 1253
Gauthier D J and Bienfang J C 1996 *Phys. Rev. Lett.* **77** 1751
Ashtakhov V, Hasler M, Kapitaniak T, Shabunin V and Anishchenko V 1998 *Phys. Rev.* E **58** 5620
Yanchuk S, Maistrenko Y, Lading B and Mosekilde E 2000 *Int. J. Bifurcation Chaos Appl. Sci. Eng.* **10** 2629
Kim S-Y and Lim W 2003 *J. Phys. A: Math. Gen.* **36** 6951
[10] Venkataramani C, Hunt B R and Ott E 1996 *Phys. Rev.* E **54** 1346
Venkataramani S C, Hunt B R, Ott E, Gauthier D J and Bienfang J C 1996 *Phys. Rev. Lett.* **77** 5361
Zimin A V, Hunt B R and Ott E 2003 *Phys. Rev.* E **67** 016204
[11] Alexander J C, Yorke J A, You Z and Kan I 1992 *Int. J. Bifurcation Chaos Appl. Sci. Eng.* **2** 795
Ott E, Sommerer J C, Alexander J C, Kan I and Yorke J A 1993 *Phys. Rev. Lett.* **71** 4134
Sommerer J C and Ott E 1993 *Nature* **365** 136
Ott E, Alexander J C, Kan I, Sommerer J C and Yorke J A 1994 *Physica* D **76** 384
Heagy J F, Carroll T L and Pecora L M 1994 *Phys. Rev. Lett.* **73** 3528
[12] Jalnine A and Kim S-Y 2002 *Phys. Rev.* E **65** 026210
[13] Kim S-Y, Lim W, Ott E and Hunt B 2003 *Phys. Rev.* E **68** 066203
[14] Kim S-Y and Kook H 1993 *Phys. Rev.* A **48** 785
[15] Kim S-Y, Lim W and Kim Y 2002 *Prog. Theor. Phys.* **107** 2
[16] Lim W and Kim S-Y 2004 *J. Korean Phys. Soc.* **44** 510 (Proc. 12th Thermal and Statistical Physics Workshop)
[17] Pikovsky A S and Feudel U 1995 *Chaos* **5** 1 (See equation (13) for the definition of the phase sensitivity exponent)